buildings

MDPI

Article

Comparison of Temperature Profiles of Aged and Fresh Larch Timber Beams Exposed to Radiant Heat Source

Dominik Špilák and Andrea Majlingova *

Department of Fire Protection, Faculty of Wood Sciences and Technology, Technical University in Zvolen, 960 01 Zvolen, Slovakia; xspilakd@is.tuzvo.sk

* Correspondence: majlingova@tuzvo.sk; Tel.: +421-455-206-025

Abstract

Historic timber buildings rely heavily on naturally aged wood. However, the influence of long-term environmental exposure on the thermal behavior and fire performance of such structural members remains insufficiently understood. This study evaluates the effect of natural aging on heat transfer, charring development, and the phase-change interval of free water in larch wood (*Larix decidua*). Medium-scale radiant panel tests were conducted on fresh and naturally aged timber beams. Internal temperatures were recorded at multiple depths and analyzed using derivative-based T-history methods. The temperature profiles of aged and fresh larch were highly comparable, exhibiting a strong correlation (R^2 = 0.89). Aged wood, characterized by a slightly higher density, showed shallower thermal gradients and a marginally lower average charring rate (0.63 mm·min^{-1}) compared with fresh wood (0.65 mm·min^{-1}). In both materials, the charring rate decreased with depth. The phase-change interval of free water differed markedly: fresh wood showed water evaporation between 107.8–142.1 °C, whereas aged wood exhibited an earlier and narrower interval (93.6–116.3 °C), indicating facilitated dehydration due to microstructural degradation. Overall, natural aging did not significantly impair fire-relevant thermal properties, suggesting that aged larch retains charring resistance comparable to that of fresh wood and can reliably perform in passive fire protection applications for heritage structures.

Keywords: aged wood; historical building; charring rate; moisture content; phase change interval

1. Introduction

Historic timber buildings represent an irreplaceable cultural heritage that documents the craftsmanship, architectural styles and living conditions of past generations. However, their construction of combustible materials, often without modern fire protection measures, makes them highly vulnerable to fires [1–4]. The loss of such a building results not only in material damage, but also in the irreversible loss of the historical memory. From a fire safety perspective, these structures therefore require special attention [5–7]. Protecting historic wooden buildings presents a complex technical challenge, as modern fire protection measures may compromise architectural authenticity or introduce defects in structural elements [8]. Consequently, fire protection of historic wooden buildings often relies on passive fire safety, based on the inherent fire resistance of structural elements, which is strongly dependent on their cross-sectional dimensions [3].

Historical wooden buildings are often recognized as cultural heritage and are frequently listed on the UNESCO World Heritage List [8]. Their technological design reflects

Check for updates

Academic Editor: Tomasz Sadowski

Received: 4 December 2025
Revised: 27 December 2025
Accepted: 9 January 2026
Published: 11 January 2026

Copyright: © 2026 by the authors. Licensee MDPI, Basel, Switzerland. This article is an open access article distributed under the terms and conditions of the Creative Commons Attribution (CC BY) license.

regional construction traditions and the availability of materials at the time of construction [1,9]. Their construction relied on simple but effective principles. Typically, a single wooden beam formed the basis for constructing log walls, column-and-frame systems, roof trusses, floors, and ceilings [8,10–12]. The selection of wood species was primarily governed by local availability, the function of the structural element and durability requirements [1,9].

Timber structures are often perceived as significantly more vulnerable to fire than constructions made of masonry, concrete, or steel. However, this perception does not fully reflect current understanding in fire safety engineering. Timber exhibits a predictable and well-documented response under fire exposure. When subjected to thermal loading, the temperature within the cross-section increases, leading to pyrolysis, combustion, and the formation of a charred layer on the exposed surface [13]. During fire exposure, distinct zones develop within the timber cross-section: the charred layer, the degraded wood layer and the intact wood layer. From a structural fire resistance perspective, the intact wood layer is critical, as it is the only one that can fully transfer the load caused, for example, by the weight of the structure [14]. From a structural fire resistance perspective, the intact wood layer is critical, as it is the only zone capable of reliably transferring mechanical loads during a fire.

According to Eurocode 5 [15], wood gradually loses mechanical strength as temperature increases above 20 °C. At 100 °C, wood may lose approximately 35% of its tensile strength, and at 300 °C, strength reduction can approach 100%, as reported by several authors [16–23]. The temperature range between 20 and 300 °C is therefore commonly referred to as the degraded wood layer. Eurocode 5 [15] also defines 300 °C as the conventional charring temperature, above which the charred layer is assumed to form. However, numerous studies have shown that the actual charring temperature may differ from this standardized value [5,24–27]. Pinto et al. [28] described the charred layer is a black, porous solid consisting predominantly of elemental carbon. Previous studies indicate that also the thermal conductivity of wood char is generally lower than that of intact wood at moderate temperatures; however, at temperatures exceeding approximately 600 °C, an increase in thermal conductivity may occur due to structural changes within the char layer [15,29–41]. Such high temperatures are typically confined to the outer char region during fire exposure and therefore have a limited influence on heat transfer within the remaining uncharred cross-section [42].

The lower temperature limit of 20 °C for the degraded wood layer specified in Eurocode 5 [15] is not explicitly justified. Wood does not melt; instead, its primary components soften when exposed to elevated temperatures prior to decomposition [43]. For lignin, softening occurs at temperatures above approximately 55 °C [44–46]. White [47] reported that a permanent reductions in wood strength begin at temperatures above 65 °C [48]. The thickness of the degraded wood layer is not constant and depends on factors such as heat flux, wood density, thermal conductivity and exposure duration. In general, the degraded wood layer increases with fire exposure time and progressively advances into the wood cross-section [49,50].

The formation and progression of the char layer are influenced by several material-related parameters, most notably wood density, thermal conductivity, and moisture content [34]. According to Bartlett et al. [34], wood with higher density chars more slowly due to the greater amount of material undergoing pyrolysis, a finding that has been confirmed by other studies [40,51–54]. These authors also reported that the charring rate decreases with increasing wood density.

Thermal conductivity of wood is strongly influenced by both density and moisture content [34,55–58]. Çavuş et al. [55] and Jang and Kang [56] demonstrated that thermal conductivity increases with increasing wood density, with Çavuş et al. [55] reporting a

linear relationship. Bartlett et al. [34] observed that lower density wood exhibits a faster temperature rise near the exposed surface due to lower thermal conductivity, whereas higher-density wood shows higher through-thickness temperatures and increased charring rates as a result of shallower thermal gradients [34,50].

During the phase change of water, a substantial portion of the supplied heat is consumed by evaporation rather than by an increase in temperature, which effectively retards heat transfer. As a result, wood with higher moisture content generally exhibits lower temperatures under identical heat flux conditions. Moisture content therefore also influences the extent of charring and the residual load-bearing capacity of timber elements.

Moisture content significantly affects heat transfer in wood up to the temperature at which water evaporation is complete. Several studies [57–61] have shown that thermal conductivity increases with increasing moisture content, either linearly or according to second-order equations [61]. During the phase change of water, a substantial portion of the supplied heat is consumed by evaporation rather than by an increase in temperature [4–6,37,40,51,62–65], which effectively retards heat transfer. As a result, wood with higher moisture content generally exhibits lower temperatures under identical heat flux conditions [40,45,49,51,63–66]. Moisture content therefore also influences the extent of charring and the residual load-bearing capacity of timber elements [49].

Long-term exposure to natural environmental conditions represents another important factor influencing the thermal behavior and charring characteristics of wood. The effects of sunlight, rain, temperature changes, mold and other factors causing natural aging of wood have leads to changes in wood material properties [5,6,67–69]. Kolsoom et al. [8] reported that microalgae growth may promote pyrolysis processes in wood [70]. Deng et al. [5] observed that natural aging increased porosity and damaged the cellular structure of pine wood, resulting in a reduction in ignition temperature by 15.2 °C compared with fresh wood. They further reported that aged pine formed a dense char layer during combustion, which reduced the heat release rate.

Song et al. [6] reported densities of 0.42 g·cm^{-3} for aged pine and 0.64 g·cm^{-3} for fresh pine, with aged wood exhibiting higher thermal diffusivity. They also emphasized the importance of moisture content in governing the thermal response of both aged and fresh wood. Zhao et al. [4] demonstrated that aged wood samples (elm, pine, and aspen) exhibited higher exothermic energy release than fresh samples, indicating increased susceptibility to combustion and potentially higher fire risk. Their results further showed that aged wood possesses thermal conductivity characteristics distinct from those of fresh wood.

The divergent conclusions reported in previous studies regarding the influence of aging on density, thermal diffusivity, and heat release rate can be attributed to differences in wood species, service environments, aging mechanisms, and experimental scale. While small-scale material tests tend to emphasize microstructural or chemical changes, medium-scale experiments reflect the integrated thermal response of structural elements. Consequently, aging-related changes observed at the material level do not necessarily translate into significant differences in temperature development or charring rate at the beam scale investigated in the present study.

The contribution of the present study lies in extending established thermal analysis and derivative-based evaluation methods to naturally aged structural timber subjected to realistic service conditions, thereby bridging the gap between laboratory-scale material studies and the fire performance of timber elements in historic buildings. Naturally aged wood, which integrates long-term environmental exposure, moisture cycling, and service-induced microstructural changes, is rarely available for controlled experimental investigation. By examining such material at a medium scale under sustained radiant heating, the study provides fire-relevant thermal data that reflect the actual condition

of load-bearing timber in heritage structures and supports more informed passive fire protection and conservation strategies.

2. Materials and Methods

2.1. Medium-Scale Radiant Panel Tests

Medium-scale radiant panel tests were conducted to investigate the thermal behavior of fresh and naturally aged larch wood under controlled fire exposure. The naturally aged larch beams originated from a historical rural dwelling constructed in the 19th century. Based on archival documentation, architectural assessment, and construction typology, the timber elements are estimated to have been in continuous structural service for approximately 120–150 years prior to dismantling. This period is considered the effective duration of natural aging for the specimens investigated in this study. The naturally aged timber beams were identified as European larch (*Larix decidua*), corresponding to the same species as the fresh reference material. Species identification was performed by macroscopic anatomical examination, including evaluation of growth ring structure, resin canal distribution, and latewood–earlywood contrast, which are characteristic features of *Larix decidua*. No indications of species substitution or mixed-species construction were observed.

The experimental setup was designed to simulate real-world fire scenarios encountered in heritage buildings, particularly slow-developing fires with extended heating durations localized to single structural surfaces, using one-sided radiant heating (medium-scale radiant panel test) and to allow continuous monitoring of temperature development within the wood cross-section. The medium-scale radiant panel test is a proven tool and has been used in other studies [14,27,42,49,50,71]. The tests were complemented by derivative-based analysis of the temperature–time curves in order to identify key thermal transitions and phase change phenomena during heating.

The radiant heat source was a propane–butane-fueled ceramic panel capable of delivering stable, reproducible thermal radiation across a rectangular exposure area measuring 480 mm × 280 mm (Figure 1). The emitted energy was produced by the burning propane–butane gas with a constant flow of 15 $m^3 \cdot h^{-1}$ throughout the 60-min exposure period. Prior to each test, the panel output was verified using a calibration thermocouple array to ensure uniformity across the radiating surface.

Wooden beam specimens were mounted horizontally on a pair of aerated concrete supports inside a test chamber with thermally reflective surfaces to minimize heat loss. The front face of each beam was positioned at 130 mm from the panel, ensuring a consistent heat flux and maximizing repeatability. Only one face was exposed to radiation, enforcing a unidirectional heat flow condition consistent with surface ignition in enclosed rooms. The laboratory conditions during tests were 21 ± 1 °C with relative humidity 55 ± 1%.

The dimensions of the tested specimens were selected to represent typical cross-sectional sizes of structural timber elements found in historic buildings. All samples had a rectangular cross-section and were cut to identical lengths in order to ensure comparable thermal boundary conditions during testing. The geometry of each specimen was measured prior to testing, and dimensional variability among the aged samples was recorded.

The dimensions of the wooden beam's samples were as follows: length of 1000 mm along with a height and width of 190 mm ± 1 mm for fresh larch and 190 ± 20 mm for aged larch. The surface of the samples was untreated. Each test beam was instrumented with 10 Type K (NiCr-Ni) thermocouples (Omega Engineering Inc., Norwalk, CT, USA) inserted orthogonally into predrilled holes at depths of 10 mm, 20 mm, 40 mm, 60 mm, and 80 mm from the exposed surface (Figure 2). These thermocouples recorded internal temperatures every 10 s, using an AHLBORN ALMEMO 2290-8710 (Ahlborn Mess- und Regelungstechnik GmbH, Holzkirchen, Germany) data logger.



Figure 1. Details of the medium-scale radiant panel test and aged larch samples after exposure. Visible surface cracks are characteristic of long-term natural aging and developed or widened during thermal loading; specimens were oriented so that no major crack directly faced the radiant panel at test initiation.

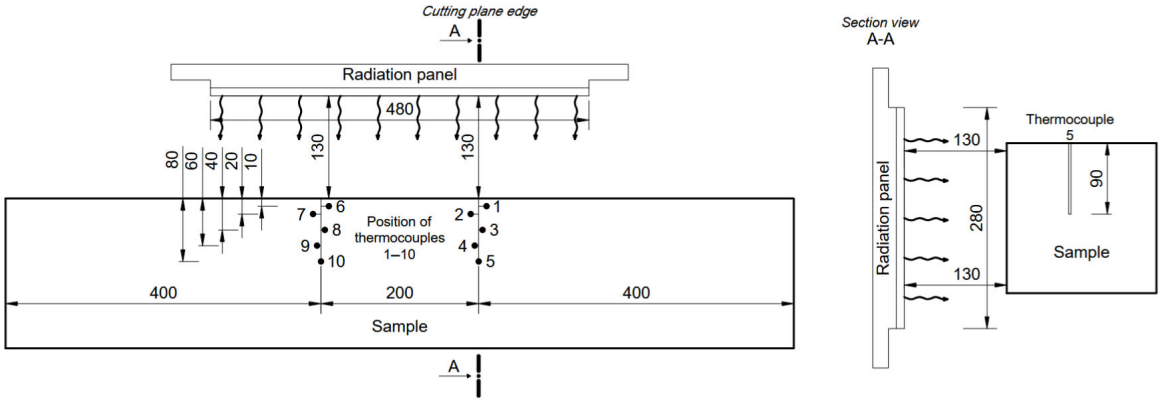


Figure 2. Distance of the test sample from the radiation panel and position of thermocouples.

2.2. Sample Geometry, Surface Condition, and Control of Distance to the Radiant Panel

Two groups of larch wood samples were used in the experimental program: fresh wood and naturally aged wood. The fresh larch samples were obtained from recently harvested timber (Technical University in Zvolen Forest Enterprise territory, Central Slovakia during the winter 2020), while the aged samples were taken from structural elements of a historical rural building dating from the nineteenth century. Based on archival documentation and architectural assessment, the aged timber elements were estimated to have been in continuous service for approximately 120–150 years prior to dismantling. Both fresh and aged samples were identified as European larch (*Larix decidua*). The service environment of the aged timber beams was typical of Central European vernacular architecture. The elements were located in interior structural positions, protected from direct solar radiation and precipitation, but subjected to long-term cyclic variations in temperature and relative humidity associated with seasonal and daily indoor climate fluctuations. Biological degradation was limited to minor surface effects, and no chemical preservation treatments were

identified. Consequently, the aging of the wood reflects combined effects of prolonged service time and natural indoor environmental exposure rather than extreme weathering.

To ensure material homology between fresh and aged wood, key physical properties relevant to heat transfer were compared prior to testing. The oven-dry density of fresh larch was 489.9 kg·m^{-3}, while the density of aged larch was 494.7 kg·m^{-3}, indicating a negligible difference well within the natural variability range reported for larch wood. Initial moisture contents were similarly close (10.0% for fresh wood and 9.7% for aged wood). These results confirm that both materials are comparable in terms of fundamental physical parameters governing thermal behavior. The cross-sectional height and width varied within ±20 mm due to long-term weathering and manual shaping during the original construction. In contrast, fresh larch beams were machine-cut to uniform dimensions. To ensure comparability between the two material conditions, several measures were implemented:

1. Control of distance to the radiant panel:

The front surface of each beam was aligned at a distance of 130 ± 1 mm from the radiant panel using a dual-point mechanical alignment jig. The jig ensured that geometric irregularities away from the heated face (rear and lateral sides) did not influence the heat flux received by the exposed surface.

2. Alignment of cracks relative to heat exposure:

The naturally aged timber beams exhibited surface and internal cracks resulting from long-term cyclic moisture loading and shrinkage during their service life. Prior to testing, particular attention was paid to the orientation of these defects. All aged specimens were positioned so that the exposed surface facing the radiant panel was free of major pre-existing cracks, ensuring that no continuous crack directly faced the heat source at the beginning of the test. This arrangement was adopted to minimize the potential for artificially accelerated heat penetration caused by preferential heat flow along open cracks.

3. Geometric influence on heat flux:

Although the aged beams deviated slightly in total cross-sectional dimensions, the exposed surface area differed by less than 5% compared with fresh beams. Considering that the heat flux from the radiant panel was uniform over an area larger than the specimen face, these variations did not measurably affect the incident energy density.

4. Representativeness for historical structures:

The geometric and surface irregularities of aged beams are characteristic of timber in existing heritage buildings. Therefore, their inclusion enhances the practical representativeness of the experimental results while maintaining methodological control of the primary heat-transfer boundary condition.

2.3. Determining the Interval of Phase Change of Water Contained in Wood

To determine the phase change interval of water contained in wood, average temperature curves were used where a temperature of 300 °C was reached. These temperature curves were used to determine the starting and ending point of the phase change interval according to the T-history method [42,72]. The average temperature curves were modified in MATLAB R2024a (MathWorks, Natick, MA, USA) software using the application "Data Cleaner". The "Smooth Data" function with parameters "Local quadratic regression" with smoothing factor in the range of 0.05–0.15 was used to smooth the curve. The goal was to smooth the curves in such a way that it was possible to clearly determine the inflection points, the minimum of the second derivative and the maximum of the first derivative.

Subsequently, curves of the first and second derivatives have been created for selected smooth temperature profiles, from which the minimum of the second derivative (t1),

the inflection point (t2) and the maximum of the first derivative (t3) were determined using MATLAB software. Using the intersections of the tangents, the starting and ending temperature of the phase change interval was determined.

2.4. Temperature and Charring Comparison

The results of the medium-scale radiant panel tests were processed into graphs and compared with each other. First, the records from the fresh larch were processed and graphs of the temperature course at individual depths were created. Six measurements were processed with, for which a curve showing the average values was created. Graphs showing the standard deviation of individual measurements were also created. Subsequently, the results for the aged larch were processed in the same way.

The comparison of temperature curves was based on the comparison of average temperatures of fresh and aged larch at individual depths. The curves of average values were compared with each other using the coefficient of determination R^2 in MATLAB (MathWorks, Inc., Natick, MA, USA) software. The charring rate, density and initial moisture content of the wood at the beginning of the test were also compared with each other.

2.5. Number of Replicates and Evaluation

A total of six replicate tests were performed for fresh larch beams and five replicate tests for aged larch beams. All tests followed identical heating protocols and instrumentation layouts. The number of replicates was selected to ensure stable statistical interpretation while respecting the limited availability of historically sourced aged timber.

Evaluation included:

- Calculation of mean temperature curves for each depth;
- Computation of standard deviation (SD) envelopes;
- Evaluation of similarity between fresh and aged wood using the coefficient of determination (R^2);
- Verification that the SD values for both fresh and aged groups remained within expected ranges for wood subjected to thermal loading [27,49,62].

Although aged beams showed higher variability, primarily due to natural heterogeneity and structural cracks, this variability remained within the bounds reported in comparable studies of naturally aged wood [4–6,73]. The nearly identical charring rates and closely correlated temperature curves confirm that the number of samples provides sufficient statistical robustness for comparing the two material conditions.

3. Results

3.1. Results: Fresh Larch

The results of medium-scale radiant panel tests on fresh larch are present on Figure 3. A total of six replicate tests were performed for fresh larch. The charring temperature defined by Eurocode 5 (300 °C) [15] was reached during the entire test period only at depths of 1 and 2 cm at times 780 and 1940 s. These time-temperature curves are therefore also suitable for determining the interval of phase change of water contained in wood. Although several authors [5,24–27] argue that the 300 °C limit does not always coincide with the physical char front, the EC5 value was used in this study to retain consistency with design practice.

The standard deviation graphs (Figure 4) showed a relatively low dispersion of the measured data. The maximum standard deviation from all measurements and depths was found at a depth of 1 cm and had a value of 53.3 °C, which represented 11.3% of the average value. The average values of the standard deviations decreased with increasing depth for 1 cm—5.3%, 2 cm—3.9%, 4 cm—0.8%, 6 cm—0.6% and for 8 cm—0.7%.

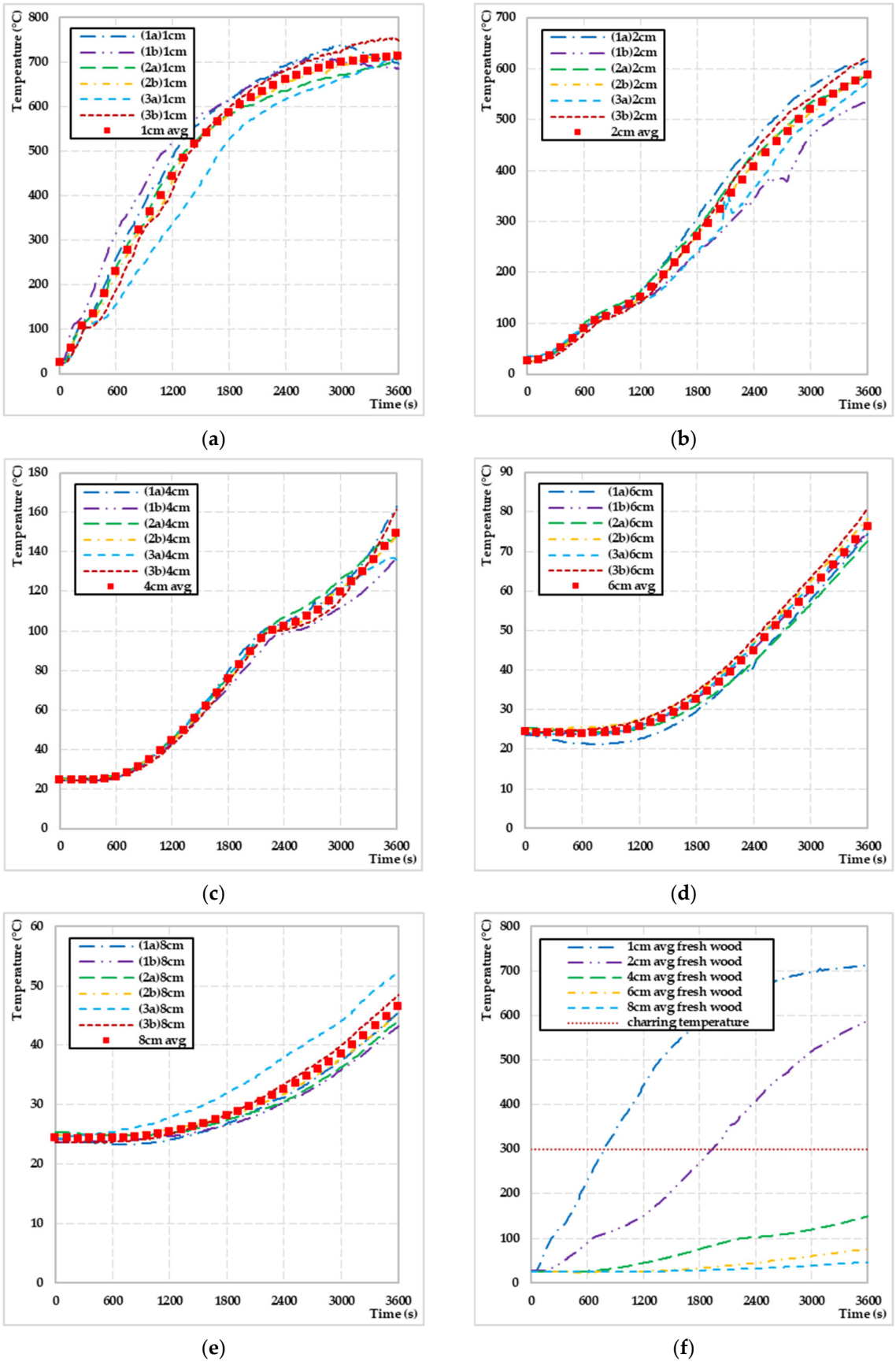
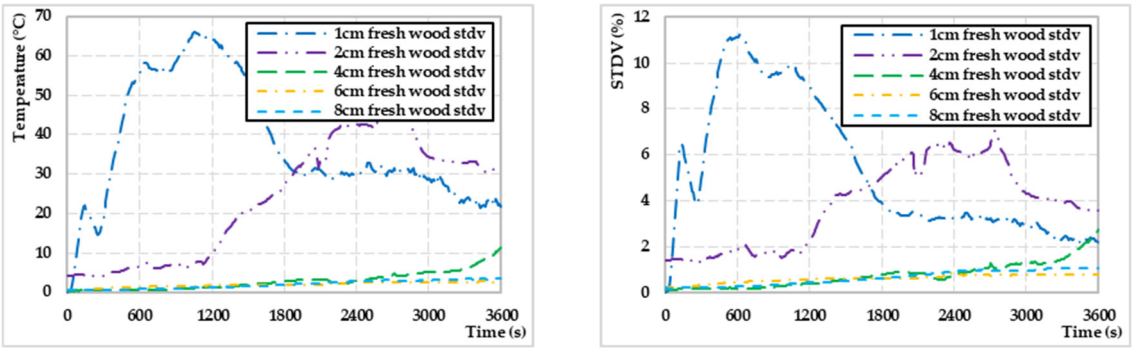


Figure 3. Temperature curves from medium-scale radiant panel tests of fresh larch: (**a**) 1 cm depth; (**b**) 2 cm depth; (**c**) 4 cm depth; (**d**) 6 cm depth; (**e**) 8 cm depth; (**f**) Comparison of average temperature curves.



(**a**) (**b**)

Figure 4. Standard deviation of average temperature curves from medium-scale radiant panel tests of fresh larch: (**a**) Standard deviation expressed by temperature; (**b**) Standard deviation expressed in percentage.

From the time-temperature curves it is possible to determine the average charring rate of fresh larch thanks to isotherm line 300 °C according to Eurocode 5 [15]. At a depth of 0 to 1 cm the rate reached 0.79 mm·min^{-1} and at a depth of 1 to 2 cm 0.52 mm·min^{-1} which is a decrease of 34.5%.

3.2. Results: Aged Larch

The results of medium-scale radiant panel tests on aged larch are present on Figure 5. A total of five replicate tests were performed for aged larch. The charring temperature defined by Eurocode 5 (300 °C) [15] was reached during the entire test period only at depths of 1 and 2 cm at times 870 and 1930 s. These time-temperature curves are therefore also suitable for determining the interval of phase change of water contained in wood. The standard deviation graphs (Figure 6) showed an increased dispersion of the measured data with increasing time. The maximum standard deviation from all measurements and depths was found at a depth of 4 cm and had a value of 145.0 °C, which represented 28.9% of the average value. The average values of the standard deviations were for 1 cm—6.2%, 2 cm—10.4%, 4 cm—7.5%, 6 cm—1.9% and for 8 cm—0.3%.

From the temperature course it is possible to determine the average charring rate of aged larch thanks to isotherm line 300 °C according to Eurocode 5 [15]. At a depth of 0 to 1 cm the rate reached 0.69 mm·min^{-1} and at a depth of 1 to 2 cm 0.57 mm·min^{-1} which is a decrease of 17.9%.

3.3. Phase Change Interval

The temperature curves show that a phase change of the water contained in the wood occurred at a depth of 1, 2 and 4 cm based on the assumption that the phase change of water occurs at a temperature of around 100 °C. However, to use the T-history method according to Zhang et al. [72], a higher temperature is required. For this reason, only average time-temperature curves from the depth of 1 cm and 2 cm from aged and fresh larch wood were used. The average values of "avg 1 cm" and "avg 2 cm" were modified in MATLAB software using the application "Data Cleaner". The "Smooth Data" function with parameters "Local quadratic regression" with 0.05 and 0.15 smoothing factor was used for to smooth the average time-temperature curves from the depth of 1 cm, respectively, 2 cm curve. Coefficient of determination R^2 had a value of 0.9995 in all cases.

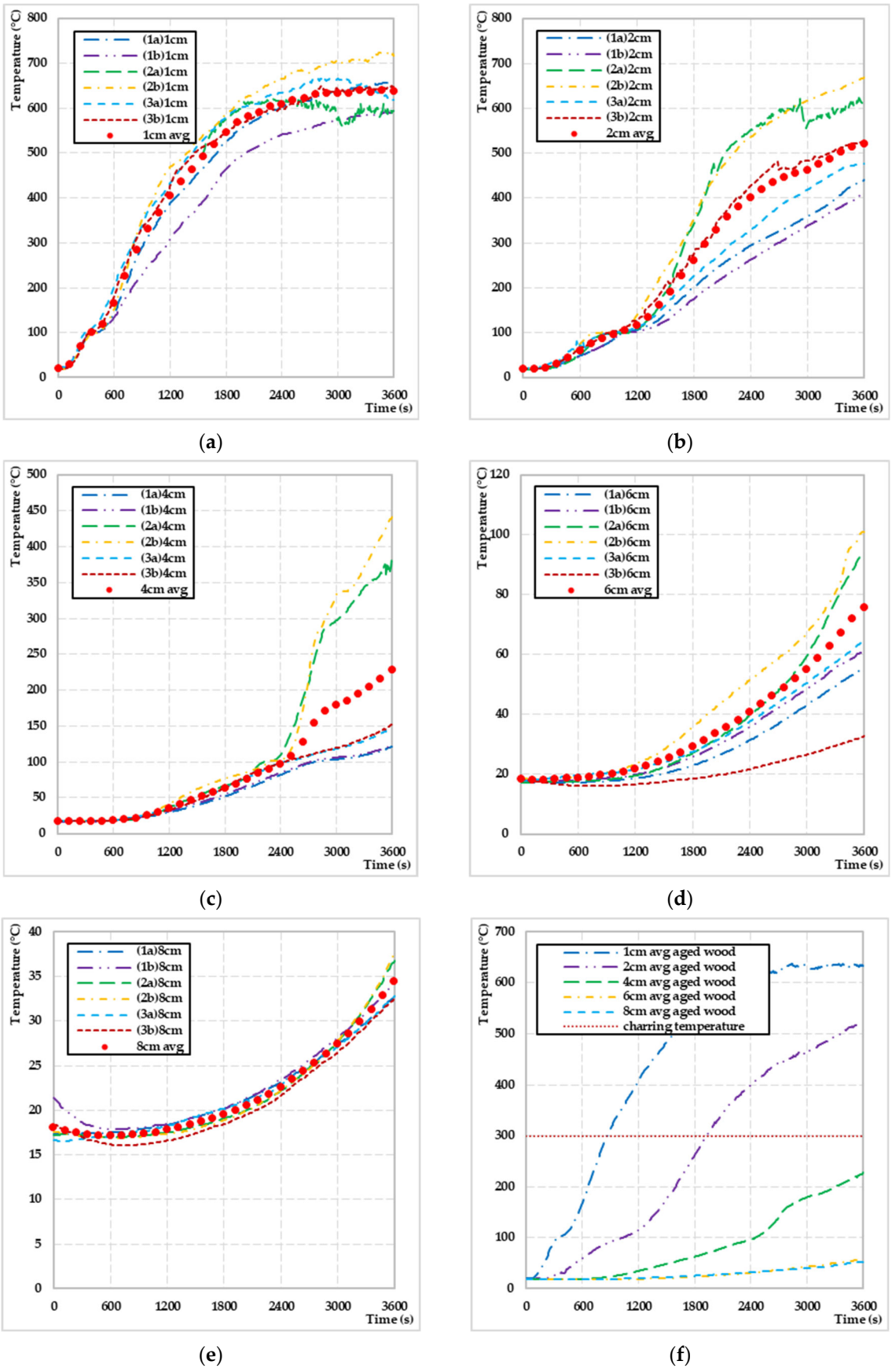
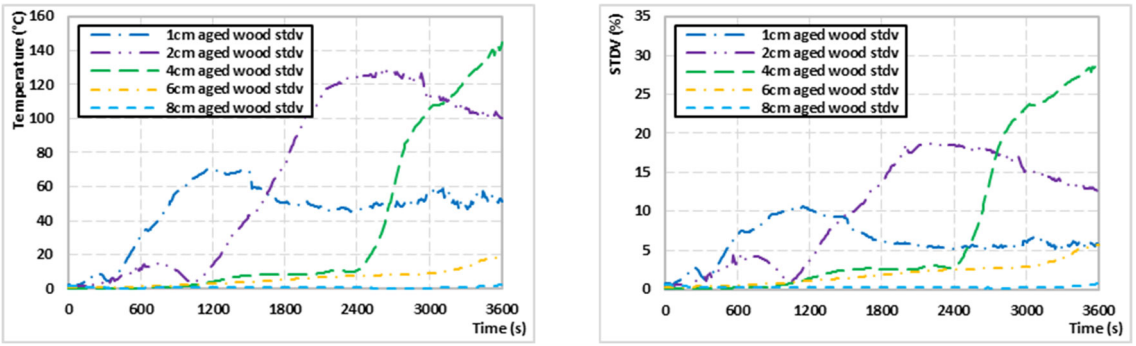


Figure 5. Temperature curves from medium-scale radiant panel tests of aged larch: (**a**) 1 cm depth; (**b**) 2 cm depth; (**c**) 4 cm depth; (**d**) 6 cm depth; (**e**) 8 cm depth; (**f**) Comparison of average temperature curves.



(**a**) (**b**)

Figure 6. Standard deviation of average temperature curves from medium-scale radiant panel tests of aged larch: (**a**) Standard deviation expressed by temperature; (**b**) Standard deviation expressed in percentage.

Subsequently, curves of the first and second derivatives were made for time-temperature curves at a depth of 1 and 2 cm, from which the minimum of the second derivative (t1), the inflection point (t2) and the maximum of the first derivative (t3) were determined using MATLAB software. The values of t1–t3 above 150 °C do not correspond to water evaporation but indicate the end points of mathematical tangents used by the T-history method [72]. Only the intersections of tangents were used to determine the physical phase-change interval. For the temperature curves of fresh wood at a depth of 1 cm, t1 = 94.5 °C, t2 = 121.8 °C and t3 = 196.0 °C (Figure 7a). For the temperature curves of fresh wood at a depth of 2 cm, t1 = 98.0 °C, t2 = 116.4 °C and t3 = 244.6 °C (Figure 7b). For the temperature curves of aged wood at a depth of 1 cm, t1 = 93.0 °C, t2 = 103.1 °C and t3 = 195.3 °C (Figure 7c). For the temperature curves of aged wood at a depth of 2 cm, t1 = 85.9 °C, t2 = 97.8 °C and t3 = 251.5 °C (Figure 7d).

For fresh wood tangents of points were generated as follows (Figure 8a,b): $y = 0.38236 \cdot x + 17.9123$, $y = 0.209225 \cdot x + 59.0269$, $y = 0.44085 \cdot x - 33.2197$ for 1 cm depth and $y = 0.123095 \cdot x + 16.6987$, $y = 0.07444 \cdot x + 52.3795$, $y = 0.214555 \cdot x - 115.874$ for 2 cm depth. For aged wood tangents of points were generated as follows (Figure 8c,d): $y = 0.29375 \cdot x + 4.7875$, $y = 0.09875 \cdot x + 65.6875$, $y = 0.46 \cdot x - 104.3$ for 1 cm depth and $y = 0.083335 \cdot x + 17.5319$, $y = 0.06417 \cdot x + 34.3467$, $y = 0.313335 \cdot x - 300.286$ for 2 cm depth.

Using the intersections of the tangents, the temperatures of the beginning and end of the phase change were determined (Figure 8a–d). The temperature intervals corresponding to the phase change of free water, derived using the T-history method, are summarized in Table 1 for both fresh and aged wood.

Table 1. Phase change interval of free water in fresh and aged larch.

Material	Depth (cm)	Phase Change Start (°C)	Phase Change End (°C)
Fresh larch	1	108.7	142.4
	2	107.0	141.8
	Average	107.8	142.1
Aged larch	1	96.5	112.2
	2	90.7	120.5
	Average	93.6	116.3

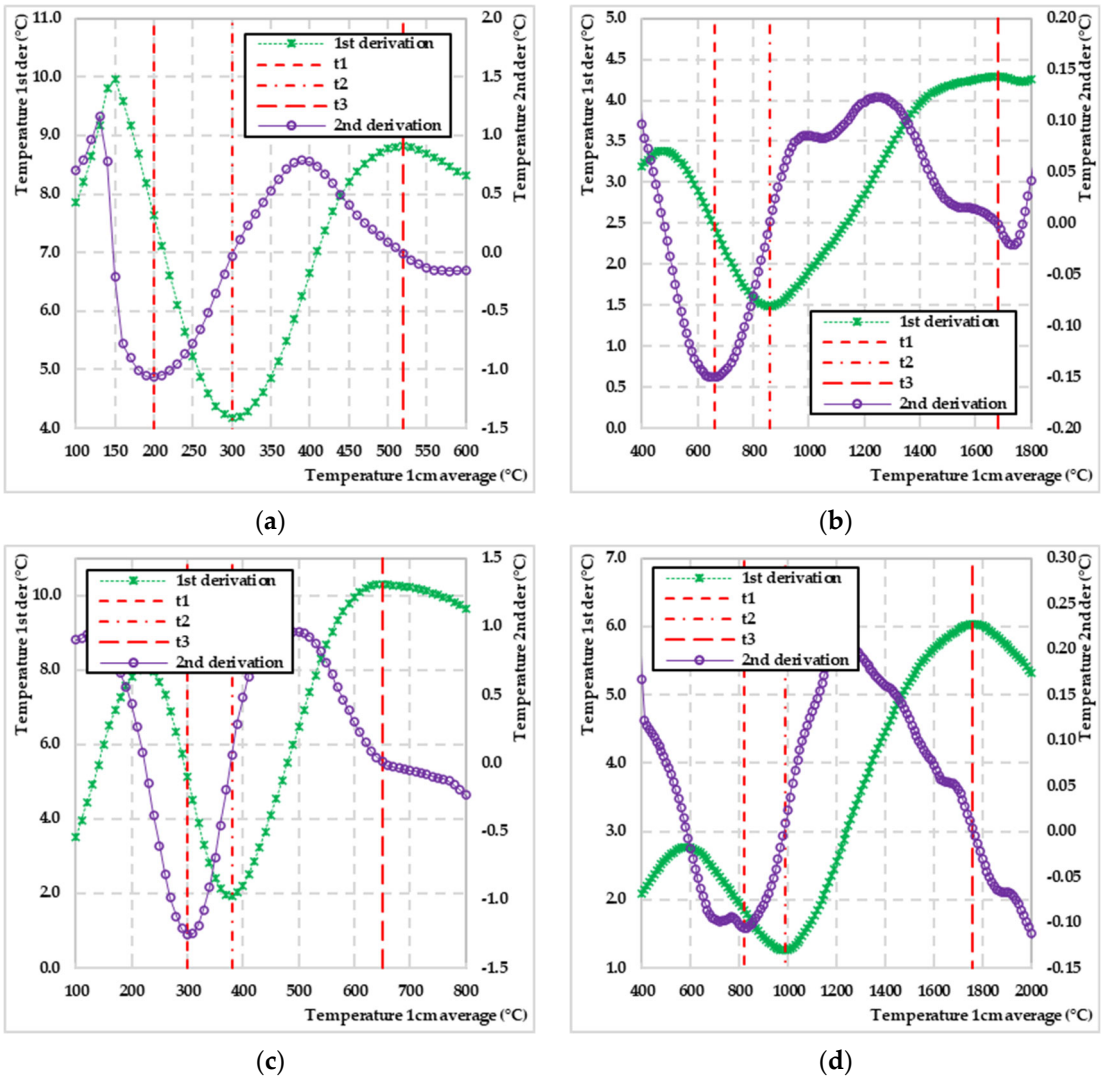


Figure 7. Curves of first and second derivation of smooth time-temperature curves: (**a**) Fresh wood 1 cm depth; (**b**) Fresh wood 2 cm depth; (**c**) Aged wood 1 cm depth; (**d**) Aged wood 2 cm depth.

It is also possible to derive the average phase change line movement rate according to phase change interval calculation. Form fresh wood at a depth of 0 to 1 cm the rate reached 3.00 mm·min^{-1}, at a depth of 1 to 2 cm 1.36 mm·min^{-1} and at a depth of 2 to 4 cm 0.76 mm·min^{-1}. The rate thus decreases from the initial maximum value by 54.5% and subsequently by another 44.3%. For aged wood at a depth of 0 to 1 cm the rate reached 1.71 mm·min^{-1}, at a depth of 1 to 2 cm 0.89 mm·min^{-1}. The rate thus decreases from the initial maximum value by 48.5%.

3.4. Results: Comparison of Aged and Fresh Larch from Medium-Scale Radiant Panel Tests

For improved clarity and direct comparison, the key physical and fire-relevant parameters of fresh and aged larch are summarized in Table 2. The tabulated presentation facilitates a concise evaluation of similarities and differences between the two material conditions.

A comparison of the temperature curves of fresh and aged wood showed the similarity of the average temperature curves (Figure 9), with aged wood reaching lower temperatures in the depth during the test, except at a depth of 4 cm, where one aged-wood specimen developed a surface crack during heating, temporarily accelerating heat penetration and causing a localized temperature increase. During testing, one aged wood specimen developed a surface crack as a result of thermal shrinkage and internal stress redistribution. This

crack formation occurred at elevated temperature and led to a localized increase in heat penetration, which was reflected by a temporary rise in temperature at a depth of 4 cm. This behavior explains the reduced coefficient of determination (R^2 = 0.76) observed at this depth compared with other measurement positions.

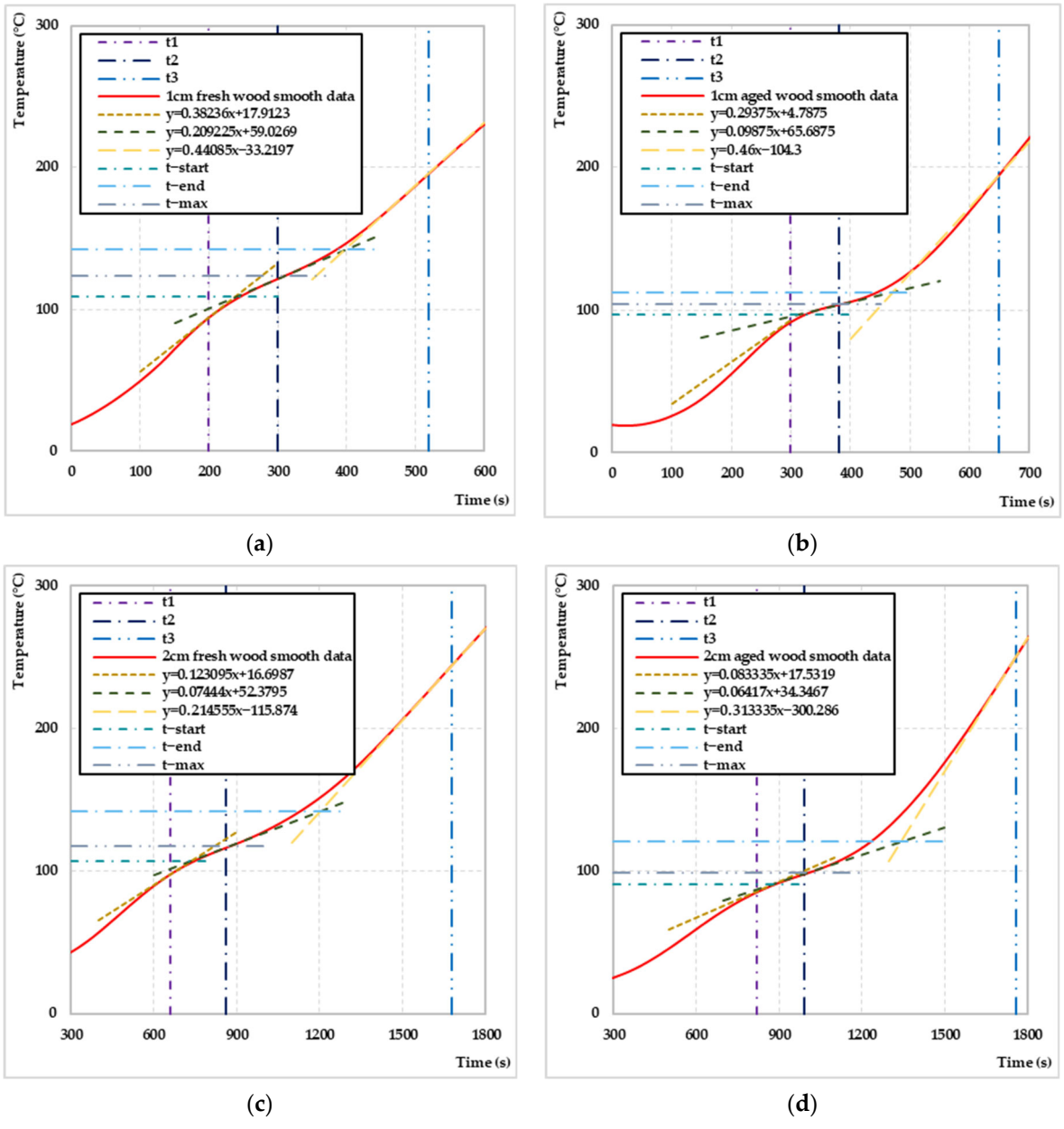
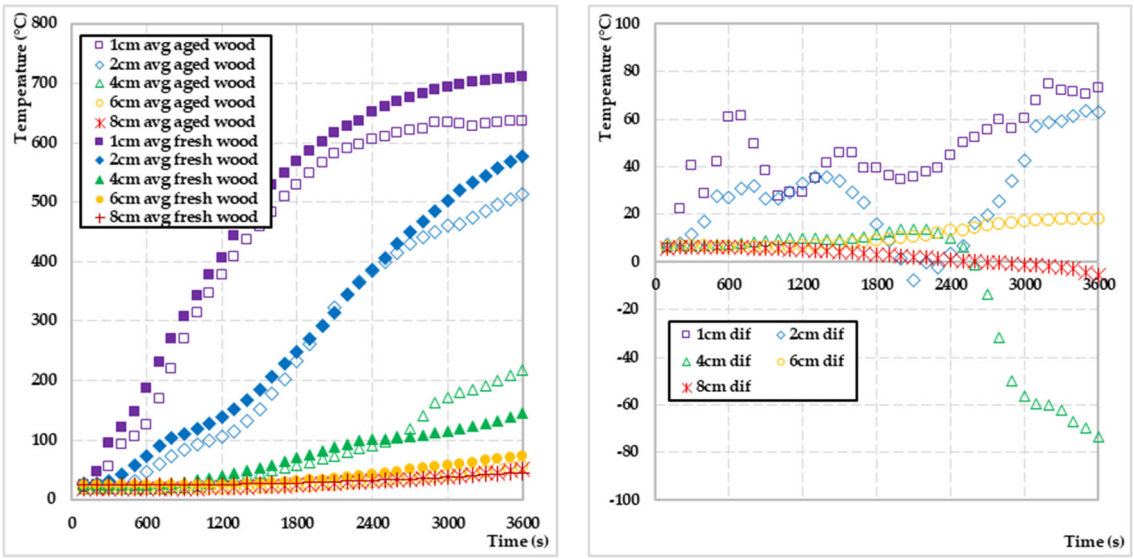


Figure 8. Tangents of points and phase change interval of smooth time-temperature curves: (**a**) Fresh wood 1 cm depth; (**b**) Fresh wood 2 cm depth; (**c**) Aged wood 1 cm depth; (**d**) Aged wood 2 cm depth.

Table 2. Physical properties of fresh and aged larch prior to testing.

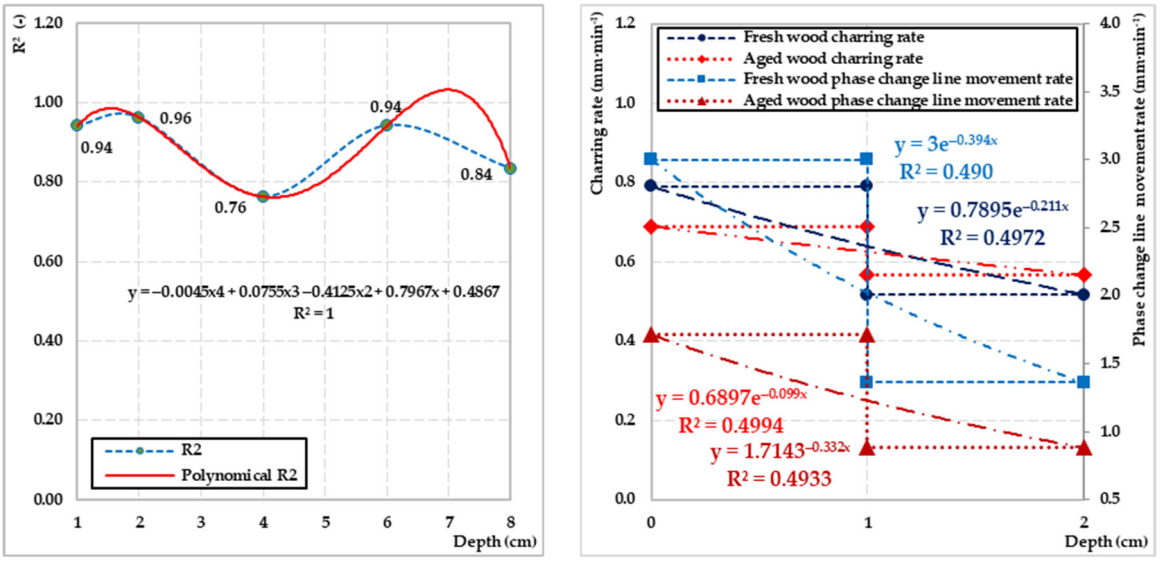
Parameter	Fresh Larch	Aged Larch
Species	*Larix decidua*	*Larix decidua*
Estimated service life (years)	–	120–150
Oven-dry density (kg·m^{-3})	489.9	494.7
Initial moisture content (%)	10.0 ± 0.1	9.7 ± 0.3
Visible cracks before testing	None	Present (natural aging)
Number of specimens	6	5



(**a**) (**b**)

Figure 9. Comparison of average temperature curves from medium-scale radiant panel tests of fresh and aged larch: (**a**) Temperature; (**b**) Deviation.

The degree of similarity of individual temperature curves between fresh and aged larch (Figure 10a) was expressed using the coefficient of determination R^2. The similarity between temperature profiles of fresh and aged larch at individual depths, expressed using the coefficient of determination (R^2), is presented in Table 3.



(**a**) (**b**)

Figure 10. Comparison of fresh and aged larch: (**a**) R^2 curves as the result of temperature curves comparison from medium-scale radiant panel tests of fresh and aged larch; (**b**) Charring rate and phase change line movement rate comparison of fresh and aged larch.

The corresponding values are best fit by a 4th order polynomial curve with R^2 of 0.99:

$$y = -0.0045 \cdot x^4 + 0.0755 \cdot x^3 - 0.4125 \cdot x^2 + 0.7967 \cdot x + 0.4867 \quad (1)$$

The average charring rates determined at different depths for fresh and aged larch are summarized in Table 4, highlighting the depth-dependent decrease observed in both materials.

Table 3. Coefficient of determination (R^2) between fresh and aged larch temperature curves.

Depth (cm)	R^2
1	0.94
2	0.96
4	0.76
6	0.94
8	0.84
Average	0.89

Table 4. Average charring rates of fresh and aged larch.

Depth Interval from Exposed Surface (cm)	Fresh Larch ($mm \cdot min^{-1}$)	Aged Larch ($mm \cdot min^{-1}$)
0–1	0.79	0.69
1–2	0.52	0.57
Mean value (0–2 cm)	0.65	0.63

A comparison of the charring rate and the phase change line movement rate showed the following. The charring rate and the phase change line movement rate decrease in both cases (Figure 10b). It is possible to construct regression curves for the indicated rates, but due to the small number of data, R^2 is relatively low. The decreasing curves do not confirm the fact stated in Eurocode 5 [15], which states that the charring rate is constant.

The results showed that aged wood does not show any signs of inferior properties in terms of its ability to withstand the effects of a radiant heat source. Although aged wood had a higher density and lower moisture content during the tests, the differences are very small and do not have a significant impact on the results of the comparison of wood species. The condition of individual wood species did not cause significant differences either. While fresh wood was compact without cracks, aged wood had several significant cracks due to its use in construction. However, they did not have a significant impact on the time-temperature results of the experiments.

4. Discussion

The results provide several important insights into how natural aging influences the thermal response of larch wood. Detailed numerical comparisons of physical properties, charring rates, phase change intervals, and temperature curve similarity are provided in Tables 1–4, allowing the discussion to focus on interpretation rather than repetition of quantitative results.

In this study, aged larch exhibited a slightly higher density than fresh wood, which differs from observations reported for pine by Song et al. [6] and for other species by Li et al. [73], who found that long-term environmental exposure generally reduces density due to microstructural degradation. However, the density of larch wood varies widely depending on site conditions, soil quality, and climatic factors [74,75], making it plausible that the original density of the aged material was higher before weathering. Therefore, natural variability rather than aging effects likely explains the density relationship observed here.

Comparative data for other softwood species, such as pine, are available in the literature; however, direct quantitative comparison is limited by differences in specimen geometry, heating configuration (e.g., radiant vs. furnace exposure), and evaluation methodology, all of which can substantially affect heat transfer and the apparent charring rate. Accordingly, the present study focuses on a consistent experimental comparison of fresh and naturally aged larch, with qualitative reference to published results for other species where appropriate [29,34,40,51,62].

The aged larch timber examined in this study had been in service for more than a century, yet its fundamental material identity and macroscopic structure remained consistent with that of fresh larch. While long-term natural aging induces microstructural changes, including increased porosity, micro-cracking, and partial cell-wall degradation, it does not alter species identity or the characteristic cellular architecture of wood. Consequently, aged and fresh larch remain directly comparable in terms of species-dependent thermal behavior and charring characteristics, despite differences in moisture transport or microstructural integrity.

Natural aging is governed by both elapsed time and service environment, including moisture cycling, thermal exposure, biological activity, and mechanical loading history. In this study, the aged wood represents a single, well-defined indoor service environment, enabling realistic assessment of fire-related thermal behavior in historical timber. However, this limits systematic separation of individual aging mechanisms or comparison across aging durations. Such evaluation would require timber from multiple service environments or artificially aged reference materials, which is beyond the scope of the present work.

Despite identical conditioning before testing, aged wood exhibited a lower initial moisture content than fresh wood. This agrees with findings by Deng et al. [5], who showed that natural aging increases pore volume and cell-wall damage, promoting faster drying. Similar observations have been reported in studies of long-term weathering effects on wood and wood–plastic composites, where repeated cycles of moisture sorption and desorption increase permeability and crack formation [68,69,76,77]. These microstructural changes likely contributed to the earlier and narrower phase-change interval observed for aged larch in the present work.

The comparison of internal temperature development showed a strong similarity between fresh and aged wood, with R^2 values above 0.89 at most depths. Aged wood exhibited slightly lower temperatures at shallow depths (1–2 cm), which can be attributed to its reduced moisture content and accelerated release of free water vapor upon heating—an effect documented in previous studies on moisture-driven heat transfer in wood [45,49,51,62–66]. At greater depths, temperature differences diminished, and at 8 cm the aged beams showed higher temperatures, which was linked to the presence of cracks that developed during testing. Crack formation in aged timber is a well-documented consequence of long-term service and thermal exposure and represents a realistic condition in historical wooden structures. Open cracks can locally enhance convective and radiative heat transfer, disrupt uniform thermal gradients, and accelerate temperature rise at greater depths. In the present study, the influence of cracks was limited to localized effects, as evidenced by increased temperature dispersion at 4 cm depth in aged wood. Importantly, this effect did not alter the overall thermal response trends, average temperature curves, or charring rates, which remained closely comparable to those of fresh wood. These facts are consistent with previous analyses provided by Janssens and White [29], Reszka and Torero [62], and Friquin [78]. From an engineering perspective, the presence of cracks in aged timber should be considered a realistic boundary condition rather than an experimental artifact. The fact that aged larch with naturally occurring cracks exhibited charring rates and overall temperature development comparable to intact fresh wood suggests that moderate cracking does not fundamentally compromise the fire-related thermal resistance of structural timber. However, cracks may increase local variability and should be accounted for in detailed fire safety assessments of heritage structures. Details on geometric variability and crack orientation control are described in Section 2.2.

The development of the char layer showed a decreasing charring rate with depth in both fresh and aged wood. This trend has been confirmed in previous radiant heating studies [27,42,50], but it contradicts the constant charring rate prescribed in Eurocode 5 [15].

The average values measured in this study (0.65 and 0.63 mm·min^{-1} for fresh and aged wood, respectively) fall within the range reported for softwoods subjected to external heating [40,51–54,76,79]. The minimal difference between the two materials suggests that natural aging does not meaningfully accelerate or delay the charring process. Instead, density and moisture content, identified as major influencing factors by Bartlett et al. [34], Çavuş et al. [55], and Jang and Kang [56], appear to govern thermal gradients more strongly than material age.

The most notable distinction between aged and fresh larch was observed in the water phase-change interval. Fresh wood exhibited a higher temperature interval (107.8–142.1 °C), whereas aged wood showed a considerably earlier and narrower interval (93.6–116.3 °C). This behavior indicates that aged wood dehydrates more easily, which is consistent with the increased porosity and micro-cracking described by Deng et al. [5] and the repeated moisture-cycling damage documented by Fu et al. [78]. The peak evaporation temperature for fresh wood (119.0 °C) aligns closely with the general value of 115 °C reported by Bartlett et al. [34], while the lower temperatures in aged wood reflect the reduced moisture-binding capacity resulting from structural deterioration.

From an engineering perspective, these results suggest that natural aging modifies moisture transport and evaporation behavior but does not significantly degrade the charring resistance of larch wood. Prior research shows that aged wood may release more thermal energy during combustion [4,6], yet this does not necessarily translate to faster char formation at structural scales. Instead, the most critical vulnerabilities in aged timber elements arise from mechanical degradation, including cracks, reduced stiffness, and loss of cross-sectional integrity, rather than from diminished thermal performance [73]. Therefore, for heritage structures, surface maintenance and protection against moisture-induced cracking may be more important for long-term fire resistance than compensating for thermal aging effects.

The experimental results further support the validity of comparing fresh and naturally aged larch in the present study. The internal temperature profiles exhibited a high degree of similarity (average $R^2 = 0.89$), and the average charring rates differed by less than 3%. These findings indicate that any aging-related microstructural differences did not result in a fundamental change in fire-relevant thermal performance. Consequently, the observed differences, most notably in the phase change interval of free water, can be attributed to aging-induced modifications of moisture transport rather than to species heterogeneity or loss of material homology.

From a broader perspective, future research should extend the investigation to naturally aged timber originating from different service environments and aging durations to better isolate the influence of environmental exposure on thermal behavior. Integrating medium-scale fire testing with microstructural characterization and moisture transport analysis would further clarify aging-related mechanisms governing heat transfer and dehydration. In addition, coupled thermal–mechanical testing under fire exposure could improve understanding of the residual load-bearing capacity of historic timber elements and support more robust fire safety assessment of heritage structures.

5. Conclusions

This study compared the thermal behavior of fresh and naturally aged larch wood through medium-scale radiant panel tests and derivative-based analysis of thermal response. The following conclusions were drawn:

- Temperature profiles of fresh and aged larch were highly similar, with an overall coefficient of determination of $R^2 = 0.89$, indicating that natural aging does not substantially alter the heat transfer behavior of larch under radiant heating.

- Aged wood exhibited slightly shallower thermal gradients, attributable to its marginally higher density, which increased thermal conductivity within the cross-section.
- The average charring rates were nearly identical: 0.65 mm·min^{-1} for fresh wood and 0.63 mm·min^{-1} for aged wood. In both materials, the charring rate decreased with depth, contradicting the constant value assumed in Eurocode 5.
- The phase change of free water occurred earlier and over a narrower temperature range in aged wood (93.6–116.3 °C) compared with fresh wood (107.8–142.1 °C). This difference is attributed to microstructural degradation that facilitates moisture transport and accelerates dehydration.
- The confirmed species homology and close agreement in density, moisture content, temperature development, and charring rate demonstrate that naturally aged larch retains fire-relevant thermal properties comparable to those of fresh larch, supporting the validity of direct experimental comparison.

Natural aging did not result in a significant reduction in charring resistance. From a passive fire protection perspective, aged larch maintains thermal performance comparable to fresh larch, and the primary concerns in heritage structures are related more to mechanical degradation and weathering defects than to diminished fire resistance.

A limitation of this study is the restricted number of aged specimens available. Future work should include a larger sample set and microstructural analyses to better characterize moisture transport mechanisms in naturally aged timber. Another limitation is that the naturally aged specimens originate from a single service environment and aging duration. Although the investigated beams are representative of interior structural timber in historic buildings, future research should address the influence of different service environments and controlled aging periods on thermal behavior by combining field-sourced historical timber with artificial aging protocols and microstructural characterization techniques.

Author Contributions: Conceptualization, A.M.; methodology, D.Š.; software, D.Š.; validation, D.Š. and A.M.; formal analysis, A.M.; investigation, D.Š.; resources, D.Š.; data curation, D.Š.; writing—original draft preparation, A.M.; writing—review and editing, A.M. and D.Š.; visualization, D.Š.; supervision, A.M.; project administration, A.M.; funding acquisition, A.M. All authors have read and agreed to the published version of the manuscript.

Funding: This research was funded by the Slovak Research and Development Agency, grant number APVV-SK-CN-21-0002 (50%) and APVV-22-0030 (50%).

Data Availability Statement: The original contributions presented in this study are included in the article. Further inquiries can be directed to the corresponding author.

Conflicts of Interest: The authors declare no conflicts of interest.

References

1. Kolář, T.; Dobrovolný, P.; Szabó, P.; Mikita, T.; Kyncl, T.; Kyncl, J.; Sochová, I.; Rybníček, M. Wood species utilization for timber constructions in the Czech lands over the period 1400–1900. *Dendrochronologia* **2021**, *70*, 125900. [CrossRef]
2. Dufraisse, A. Post-fire studies of Notre Dame's framework: Historical and environmental wood memory of the medieval period between the 11th and 13th centuries. Birth of an interdisciplinary project. *J. Cult. Herit.* **2024**, *65*, 17–20. [CrossRef]
3. Dzidic, S.; Aktee, O.A. Fire Resistance Assessment of Timber Elements. In *New Technologies, Development and Application VIII*; Springer: Cham, Switzerland, 2025; Volume 1484, pp. 491–499. [CrossRef]
4. Zhao, J.Y.; Jiang, X.R.; Song, J.J.; Lu, S.P.; Xiao, Y.Y.; Shu, C.M. Influence of natural aging on wood combustion heat release. *Wood Sci. Technol.* **2024**, *58*, 1227–1257. [CrossRef]
5. Deng, J.; Liu, T.S.; Yao, M.; Yi, X.; Bai, G.X.; Huang, Q.R.; Li, Z. Comparative study of the combustion and kinetic characteristics of fresh and naturally aged pine wood. *Fuel* **2023**, *343*, 127962. [CrossRef]
6. Song, J.J.; Deng, J.; Zhao, J.Y.; Lu, S.P.; Ming, H.Q.; Shu, C.M. Comparative analysis of exothermic behaviour of fresh and aged pine wood. *J. Therm. Anal. Calorim.* **2022**, *147*, 14393–14406. [CrossRef]

7. Tozo Neto, J.; Ferreira, T.M. Assessing and mitigating vulnerability and fire risk in historic centres: A cost-benefit analysis. *J. Cult. Herit.* **2020**, *45*, 279–290. [CrossRef]
8. Santini, S.; Borghese, V.; Baggio, C. HBIM-Based Decision-Making Approach for Sustainable Diagnosis and Conservation of Historical Timber Structures. *Sustainability* **2023**, *15*, 3003. [CrossRef]
9. Filkova, V.; Kolar, T.; Rybnicek, M.; Gryc, V.; Vavrcik, H.; Jurcik, J. Historical utilization of wood in southeastern Moravia (Czech Republic). *Iforest-Biogeosci. For.* **2015**, *8*, 101–107. [CrossRef]
10. Marciniak, P.; Pawlak, Z.M.; Wyczalek, I. The Use of Experimental Modal Analysis in Modeling the Complex Timber Structure of a Historical Building. *Appl. Sci.* **2024**, *14*, 8517. [CrossRef]
11. Gineiko, A.; Kiviste, M. Strength- and Moisture-Related Studies of Historical Building Materials: A Case Study from Southern Estonia. *Buildings* **2024**, *14*, 3565. [CrossRef]
12. Antoine, E.; Marquer, L.; Muigg, B.; Tegel, W.; Bisson, U.; Bolliger, M.; Herzig, F.; Heussner, K.-U.; Hofmann, J.; Kontic, R.; et al. Legacy of last millennium timber use on plant cover in Central Europe: Insights from tree rings and pollen. *Sci. Total Environ.* **2024**, *922*, 171157. [CrossRef]
13. Čabalová, I.; Kačík, F.; Kačíková, D.; Oravec, M. The influence of radiant heating on chemical changes of spruce wood. *Acta Fac. Xylologiae* **2013**, *55*, 59–66.
14. Špilák, D.; Andrea, M.; Kačíková, D. *Progressive Methods for Determining the Fire Resistance of Wooden Beams*; Aleš Čeněk: Prague, Czechia, 2022; p. 162.
15. European Committee for Standardization; British Standards Institution. *Eurocode 5: Design of Timber Structure*; BSI: Brussels, Belgium, 1994.
16. Van Zeeland, I.; Salinas, J.; Mehaffey, J. Compressive strength of lumber at high temperatures. *Fire Mater.* **2005**, *29*, 71–90. [CrossRef]
17. Glos, P.; Henrici, D. Längsdruck-E-Modul von Fichtenbauholz im Temperaturbereich bis 150 °C. *Eur. J. Wood Wood Prod.* **1991**, *49*, 298. [CrossRef]
18. Schaffer, E. *Elevated Temperature Effect on the Longitudinal Mechanical Properties of Wood*; The University of Wisconsin-Madison: Madison, WI, USA, 1971.
19. König, J. *Timber Frame Assemblies Exposed to Standard and Parametric Fires. Part 2 A Design Model for Standard Fire Exposure*; Swedish Institute for Wood Technology Research: Stockholm, Sweden, 2000.
20. König, J. Structural fire design according to Eurocode 5—Design rules and their background. *Fire Mater.* **2005**, *29*, 147–163. [CrossRef]
21. Gerhards, C.C. Effect of moisture content and temperature on the mechanical properties of wood: An analysis of immediate effects. *Wood Fiber* **1982**, *14*, 4–36.
22. Kuronen, H.; Mikkola, E.; Hostikka, S. Tensile strength of wood in high temperatures before charring. *Fire Mater.* **2021**, *45*, 858–865. [CrossRef]
23. Yue, K.; Wu, J.H.; Wang, F.; Chen, Z.J.; Lu, W.D. Mechanical Properties of Douglas Fir Wood at Elevated Temperatures under Nitrogen Conditions. *J. Mater. Civ. Eng.* **2022**, *34*, 04021434. [CrossRef]
24. Parnicanová, A.; Zachar, M.; Kacíková, D. The Influence of the Heat Flux of the Infrared Heater on the Charring Rate of Spruce Wood. *Polymers* **2024**, *16*, 2657. [CrossRef]
25. Pecenko, R.; Hozjan, T. A novel approach to determine charring of wood in natural fire implemented in a coupled heat-mass-pyrolysis model. *Holzforschung* **2021**, *75*, 148–158. [CrossRef]
26. Pecenko, R.; Knez, N.; Hozjan, T.; Sejna, J.; Cabová, K.; Turk, G. On the char front temperature of beech (*Fagus sylvatica*). *Wood Sci. Technol.* **2024**, *58*, 1535–1553. [CrossRef]
27. Dúbravská, K.; Kucerová, V.; Stefková, J.; Misíkoáva, O. Charring of and Chemical Changes in Historical Wood under Thermal Loading. *Forests* **2024**, *15*, 1189. [CrossRef]
28. Pinto, E.; Machado, G.O.; Felipetto, R.P.F.; Christoforo, A.L.; Rocco Lahr, F.; Calil, C. Thermal Degradation and Charring Rate of and Wood Species. *Open Constr. Build. Technol. J.* **2016**, *10*, 450–456. [CrossRef]
29. Janssens, M.; White, R. Short communication: Temperature profiles in wood members exposed to fire. *Fire Mater.* **1994**, *18*, 263–265. [CrossRef]
30. Frangi, A. *Brandverhalten von Holz-Beton-Verbunddecken*; 3-7643-6681-8; Birkhäuser: Basel, Switzerland, 2001.
31. Maciulaitis, R.; Jefimovas, A.; Zdanevicius, P. Research of natural wood combustion and charring processes. *J. Civ. Eng. Manag.* **2012**, *18*, 631–641. [CrossRef]
32. Kamenická, Z.; Sandanus, J.; Blesák, L.; Cabová, K.; Wald, F. Methods for determining the charring rate of timber and their mutual comparison. *Wood Res.* **2018**, *63*, 583–590.
33. Wald, F.; Pokorný, M.; Horová, K.; Hejtmánek, P.; Najmanová, H.; Benýšek, M.; Kurejková, M.; Schwarz, I. *Modelování Dynamiky Požáru v Budovách*; České vysoké učení technické v Praze: Prague, Czechia, 2017.

34. Bartlett, A.I.; Hadden, R.M.; Bisby, L.A. A Review of Factors Affecting the Burning Behaviour of Wood for Application to Tall Timber Construction. *Fire Technol.* **2019**, *55*, 1–49. [CrossRef]
35. Kmiecik, K. Impact of wood species on the timber beam strength and stiffness under fire. *IOP Conf. Ser. Mater. Sci. Eng.* **2019**, *586*, 012004. [CrossRef]
36. Malaga-Tobola, U.; Lapka, M.; Tabor, S.; Nieslony, A.; Findura, P. Influence of wood anisotropy on its mechanical properties in relation to the scale effect. *Int. Agrophysics* **2019**, *33*, 337–345. [CrossRef]
37. Hu, Y.P.; Li, W.B.; Wu, S.; Wang, Y.J.; Zhong, W.Z.; Zhang, H. Experimental Study of the Anisotropic Thermal Conductivity of Spruce Wood. *Int. J. Thermophys.* **2023**, *44*, 131. [CrossRef]
38. White, R.H.; Dietenberger, M. Fire safety of wood construction. In *Wood Handbook—Wood as an Engineering Material*; Forest Products Laboratory: Madison, WI, USA, 2010; pp. 1–17.
39. Blass, H.J. *Timber Engineering: STEP 1: Basis of Design, Material Properties, Structural Components and Joints*; Centrum Hout Almere: Almere, The Netherlands, 1995.
40. Friquin, K.L. Material properties and external factors influencing the charring rate of solid wood and glue-laminated timber. *Fire Mater.* **2011**, *35*, 303–327. [CrossRef]
41. Harper, C.A. *Handbook of Building Materials for Fire Protection*; McGraw Hill LLC: Columbus, OH, USA, 2003.
42. Spilak, D.; Dubravska, K.; Majlingova, A.; Jin, C.; Xu, Q.; Jiang, L. Modification of Computer-Aided Modelling Input Data Based on Medium-Scale Fire Tests of Wooden Beams. *Bioresources* **2025**, *20*, 1230–1250. [CrossRef]
43. Beyler, C.; Hirschler, M. Thermal decomposition of polymers. In *SFPE Handbook of Fire Protection Engineering*; SFPE: Gaithersburg, MD, USA, 2002; Volume 2.
44. Etris, S.; Lieb, K.; Sisca, V.; Moore, I.; Batik, A.; Schaffer, E. Effect of Pyrolytic Temperatures on the Longitudinal Strength of Dry Douglas-Fir. *J. Test. Eval.* **1973**, *1*, 319–329.
45. Shen, D.K.; Fang, M.X.; Luo, Z.Y.; Cen, K.F. Modeling pyrolysis of wet wood under external heat flux. *Fire Saf. J.* **2007**, *42*, 210–217. [CrossRef]
46. Li, W.Y.; Sun, N.; Stoner, B.; Jiang, X.Y.; Lu, X.M.; Rogers, R.D. Rapid dissolution of lignocellulosic biomass in ionic liquids using temperatures above the glass transition of lignin. *Green Chem.* **2011**, *13*, 2038–2047. [CrossRef]
47. Fuller, J.J.; Leichti, R.J.; White, R.H. Temperature distribution in a nailed gypsum-stud joint exposed to fire. *Fire Mater.* **1992**, *16*, 95–99. [CrossRef]
48. White, R.H.; Dietenberger, M. Wood Products: Thermal Degradation and Fire. In *Encyclopedia of Materials: Science and Technology*; Elsevier: Amsterdam, The Netherlands, 2001; pp. 9712–9716. [CrossRef]
49. Spilák, D.; Majlingová, A. Progressive Methods in Studying the Charred Layer Parameters Change in Relation to Wood Moisture Content. *Polymers* **2022**, *14*, 4997. [CrossRef]
50. Spilák, D.; Majlingová, A.; Kacíková, D.; Tischler, P. Determining the Charred Layer of Wooden Beams with Finite Element Analysis Based on Enthalpy Approach. *Buildings* **2022**, *12*, 875. [CrossRef]
51. Cachim, P.B.; Franssen, J.-M. Comparison between the charring rate model and the conductive model of Eurocode 5. *Fire Mater.* **2009**, *33*, 129–143. [CrossRef]
52. Yang, T.H.; Wang, S.Y.; Tsai, M.J.; Lin, C.Y. Temperature distribution within glued laminated timber during a standard fire exposure test. *Mater. Des.* **2009**, *30*, 518–525. [CrossRef]
53. Yang, T.H.; Wang, S.Y.; Tsai, M.J.; Lin, C.Y. The charring depth and charring rate of glued laminated timber after a standard fire exposure test. *Build. Environ.* **2009**, *44*, 231–236. [CrossRef]
54. Schmid, J.; Just, A.; Klippel, M.; Fragiacomo, M. The Reduced Cross-Section Method for Evaluation of the Fire Resistance of Timber Members: Discussion and Determination of the Zero-Strength Layer. *Fire Technol.* **2015**, *51*, 1285–1309. [CrossRef]
55. Çavus, V.; Sahin, S.; Esteves, B.; Ayata, Ü. Determination of Thermal Conductivity Properties in Some Wood Species Obtained from Turkey. *Bioresources* **2019**, *14*, 6709–6715. [CrossRef]
56. Jang, E.S.; Kang, C.W. The relationship between bulk density and thermal conductivity in various korean woods. *Wood Res.* **2022**, *67*, 178–186. [CrossRef]
57. Kristák, L.; Igaz, R.; Ruziak, I. Applying the EDPS Method to the Research into Thermophysical Properties of Solid Wood of Coniferous Trees. *Adv. Mater. Sci. Eng.* **2019**, *2019*, 2303720. [CrossRef]
58. Vololonirina, O.; Coutand, M.; Perrin, B. Characterization of hygrothermal properties of wood-based products—Impact of moisture content and temperature. *Constr. Build. Mater.* **2014**, *63*, 223–233. [CrossRef]
59. Amel, L.; Zerizer, A.; Quenard, D.; Hebert, S.; Abdelkrim, C. Experimental thermal characterization of bio-based materials (Aleppo Pine wood, cork and their composites) for building insulation. *Energy Build.* **2016**, *116*, 89–95. [CrossRef]
60. Mvondo, R.R.N.; Damfeu, J.C.; Meukam, P.; Jannot, Y. Influence of moisture content on the thermophysical properties of tropical wood species. *Heat Mass Transf.* **2020**, *56*, 1365–1378. [CrossRef]

61. Zvicevicius, E.; Raila, A.; Cipliene, A.; Ziura, K. Influence of moisture on osier willow chops characteristics. In Proceedings of the 18th International Scientific Conference on Engineering for Rural Development (ERD), Jelgava, Latvia, 22–24 May 2019; pp. 1561–1567.
62. Reszka, P.; Torero, J.L. In-depth temperature measurements in wood exposed to intense radiant energy. *Exp. Therm. Fluid Sci.* **2008**, *32*, 1405–1411. [CrossRef]
63. Cachim, P.B.; Franssen, J.-M. Assessment of Eurocode 5 Charring Rate Calculation Methods. *Fire Technol.* **2010**, *46*, 169–181. [CrossRef]
64. Maraveas, C.; Miamis, K.; Matthaiou, C.E.; Maraveas, C. Performance of Timber Connections Exposed to Fire: A Review. *Fire Technol.* **2015**, *51*, 1401–1432. [CrossRef]
65. Rinta-Paavola, A.; Sukhomlinov, D.; Hostikka, S. Modelling Charring and Burning of Spruce and Pine Woods During Pyrolysis, Smoldering and Flaming. *Fire Technol.* **2023**, *59*, 2751–2786. [CrossRef]
66. Richter, F.; Rein, G. A multiscale model of wood pyrolysis in fire to study the roles of chemistry and heat transfer at the mesoscale. *Combust. Flame* **2020**, *216*, 316–325. [CrossRef]
67. Regueira, R.; Guaita, M. Numerical simulation of the fire behaviour of timber dovetail connections. *Fire Saf. J.* **2018**, *96*, 1–12. [CrossRef]
68. Liu, R.; Pang, X.; Yang, Z. Measurement of three wood materials against weathering during long natural sunlight exposure. *Meas. J. Int. Meas. Confed.* **2017**, *102*, 179–185. [CrossRef]
69. Rosu, D.; Teaca, C.-A.; Bodirlau, R.; Rosu, L. FTIR and color change of the modified wood as a result of artificial light irradiation. *J. Photochem. Photobiol. B Biol.* **2010**, *99*, 144–149. [CrossRef]
70. Azizi, K.; Moraveji, M.K.; Najafabadi, H.A. Simultaneous pyrolysis of microalgae *C. vulgaris*, wood and polymer: The effect of third component addition. *Bioresour. Technol.* **2018**, *247*, 66–72. [CrossRef]
71. Dubravska, K.; Spilak, D.; Terenova, L.; Stefkova, J. Charring Layer on a Cross-laminated Timber Panel Construction. *Acta Fac. Xylologiae Zvolen* **2019**, *61*, 109–119. [CrossRef]
72. Zhang, Y.Y.C.; Zhang, X.L.; Xu, X.F.; Lu, M.Y. Derivation of thermal properties of phase change materials based on T-history method. *J. Energy Storage* **2020**, *27*, 101062. [CrossRef]
73. Li, T.; Wu, Q.; Lu, W.; Zhang, J.; Yue, Z.; Jie, Y.; Zhang, J.; Cheng, Z.; Ji, W.; Wu, J. Effects of different accelerated aging modes on the mechanical properties, color and microstructure of wood. *J. Build. Eng.* **2024**, *98*, 111026. [CrossRef]
74. Marciszewska, K.; Szczepkowski, A.; Lachowicz, H.; Antczak, A.; Szadkowska, D.; Suchodolski, J. The physical, mechanical, and chemical properties of black cherry tree wood (*Prunus serotina* Ehrh.) and its susceptibility to fungal decomposition in areas where it is secondary and invasive: A case study in the Kampinos National Park (Poland). *Eur. J. Wood Wood Prod.* **2024**, *82*, 683–701. [CrossRef]
75. ANSYS. *Ansys Granta Data Selector*; ANSYS: Canonsburg, PA, USA, 2024.
76. Darmon, R.; Lalu, O. The fire performance of Cross Laminated Timber beams. *Procedia Manuf.* **2018**, *32*, 121–128. [CrossRef]
77. Fu, Z.Y.; Chen, J.; Zhang, Y.; Xie, F.; Lu, Y. Review on Wood Deformation and Cracking during Moisture Loss. *Polymers* **2023**, *15*, 3295. [CrossRef]
78. Friquin, K. *Charring Rates of Heavy Timber Structures for Fire Safety Design: A Study of the Charring Rates Under Various Fire Exposures Andthe Influencing Factors*; Norges Teknisk-Naturvitenskapelige Universitet: Trondheim, Norway, 2010.
79. Segerholm, B.K.; Ibach, R.E.; Wålinder, M.E.P. Moisture sorption in artificially aged wood-plastic composites. *Bioresources* **2012**, *7*, 1283–1293. [CrossRef]

Disclaimer/Publisher's Note: The statements, opinions and data contained in all publications are solely those of the individual author(s) and contributor(s) and not of MDPI and/or the editor(s). MDPI and/or the editor(s) disclaim responsibility for any injury to people or property resulting from any ideas, methods, instructions or products referred to in the content.